Neuro-Oncology Advances

6(1), vdae080, 2024 | https://doi.org/10.1093/noajnl/vdae080 | Advance Access date 30 May 2024

Imaging meningioma biology: Machine learning predicts integrated risk score in WHO grade 2/3 meningioma

Olivia Kertels[*], Claire Delbridge[*], Felix Sahm, Felix Ehret, Güliz Acker, David Capper, Jan C. Peeken, Christian Diehl, Michael Griessmair, Marie-Christin Metz, Chiara Negwer, Sandro M. Krieg, Julia Onken, Igor Yakushev, Peter Vajkoczy, Bernhard Meyer, Daniel Zips, Stephanie E. Combs, Claus Zimmer, David Kaul[†], Denise Bernhardt[†], and Benedikt Wiestler[†]

All author affiliations are listed at the end of the article

Corresponding Author: Benedikt Wiestler, MD, Department of Diagnostic and Interventional Neuroradiology, School of Medicine, Klinikum rechts der Isar, Technical University of Munich, Ismaningerstr. 22, 81675 Munich, Germany (b.wiestler@tum.de).

[*]O.K. and C.D. contributed equally as first authors.
[†]D.K., D.B., and B.W. contributed equally as senior authors.

Abstract

Background. Meningiomas are the most common primary brain tumors. While most are benign (WHO grade 1) and have a favorable prognosis, up to one-fourth are classified as higher-grade, falling into WHO grade 2 or 3 categories. Recently, an integrated risk score (IRS) pertaining to tumor biology was developed and its prognostic relevance was validated in a large, multicenter study. We hypothesized imaging data to be reflective of the IRS. Thus, we assessed the potential of a machine learning classifier for its noninvasive prediction using preoperative magnetic resonance imaging (MRI).

Methods. In total, 160 WHO grade 2 and 3 meningioma patients from 2 university centers were included in this study. All patients underwent surgery with histopathological workup including methylation analysis. Preoperative MRI scans were automatically segmented, and radiomic parameters were extracted. Using a random forest classifier, 3 machine learning classifiers (1 multiclass classifier for IRS and 2 binary classifiers for low-risk and high-risk prediction, respectively) were developed in a training set (120 patients) and independently tested in a hold-out test set (40 patients).

Results. Multiclass IRS classification had a test set area under the curve (AUC) of 0.7, mostly driven by the difficulties in clearly separating medium-risk from high-risk patients. Consequently, a classifier predicting low-risk IRS versus medium-/high-risk showed a very high test accuracy of 90% (AUC 0.88). In particular, "sphericity" was associated with low-risk IRS classification.

Conclusion. The IRS, in particular molecular low-risk, can be predicted from imaging data with high accuracy, making this important prognostic classification accessible by imaging.

Key Points

1. Machine learning classifiers are able to assess molecular risk profile in higher-grade meningiomas.
2. The integrated risk score and, in particular, the molecular low-risk group can be predicted noninvasively by radiomics.

Importance of the Study

Recently, an integrated molecular and morphologic risk score (IRS) that combines WHO grading, DNA methylation family (MF), and specific copy number variants (CNV) has been demonstrated to enhance diagnostic accuracy in meningiomas. However, this IRS has not yet been implemented in routine practice. Radiomics approaches can identify quantitative imaging information that are "hidden" within medical imaging. We explored the noninvasive prediction of IRS using magnetic resonance imaging data for WHO grade 2 and 3 meningiomas and developed a machine learning classifier to noninvasively predict the molecular risk profile. Notably, sphericity, which measures the tumor's roundness relative to a sphere, was identified as significant for IRS and for identifying low-risk patients. The noninvasive prediction of IRS, utilizing radiomics and machine learning, holds promise for revealing crucial insights and treatment decision-making, especially in patients with low-risk profiles.

Meningiomas are the most common primary central nervous system (CNS) tumors.[1] Whereas most lesions are benign (WHO grade 1) and generally have a favorable prognosis, higher-grade WHO grade 2 and 3 meningiomas are associated with higher recurrence rates and shorter overall survival.[2–4] However some WHO grade 2 and 3 meningiomas have a benign follow-up which is not readily explained by histology alone.[5,6]

In contrast enhanced magnetic resonance imaging (MRI), meningiomas show characteristic imaging features, usually leading to an accurate diagnosis. Different MRI features, for example, enhancement degree, apparent diffusion coefficient (ADC) values or peritumoral edema have been shown to distinguish between low-grade and high-grade meningioma.[7] Unlike traditional structural MRI imaging, radiomics provide quantitative imaging information and its use has been demonstrated in different brain tumors and settings with the potential of uncovering important information "hidden" in medical imaging.[8–13]

Recently, molecular markers have increasingly supplemented and synergistically enhanced the traditionally histology-based classification as well as tumor grading in many CNS tumors, including meningiomas.[14] An integrated molecular and morphologic risk score (IRS), combining WHO grading, DNA methylation family (MF) and specific copy number variants (CNV) was already suggested by Maas et al. to increase diagnostic accuracy especially in patients who are at high risk for disease progression.[14] Importantly, this IRS has been shown to be of high prognostic relevance.

However, assessing IRS requires large-scale epigenetic profiling, which might impede its widespread routine implementation. Our present multicentric study aimed to investigate the use of radiomics and machine learning to predict noninvasively IRS from preoperative MR imaging in WHO grade 2 and 3 meningiomas. To our knowledge, this is the first study to evaluate noninvasive IRS status based on radiomics and machine learning.

Patients and Methods

Ethics Statement

The present study was conducted according to the guidelines of the Declaration of Helsinki, and the retrospective analysis of data was approved by the Ethics Committees of the participating university hospitals (Berlin: EA2/059/21; Munich: 257/21 S-KK).

Patients

This retrospective analysis included a total of 160 patients with meningioma WHO grades 2 and 3 from 2 different university hospitals. Patients were retrospectively identified for (i) pathohistological diagnosis of a WHO grade 2 or 3 meningioma, (ii) available preoperative imaging (including T1w images –/+ contrast, T2w images, fluid attenuated inversion recovery [FLAIR] images), and (iii) tissue material available for IRS profiling. Clinical data were obtained from the local electronic patient records.

Neuropathological Assessment and (Epi)genetic Profiling

Tumor tissue samples were obtained from patients who underwent surgical resection. DNA was extracted from these samples using a standardized protocol, ensuring high-quality DNA suitable for subsequent analysis, as previously described.[15] DNA methylation analysis was performed using 850k EPIC Illumina Infinium Methylation Array (Illumina). DNA methylation data preprocessing and analysis involved several steps. Raw data obtained from the analysis platform were subjected to quality control measures, including filtering and normalization procedures to ensure data integrity and comparability across samples. Tumor methylation classification based on their DNA methylation profiles was done with MolecularNeuropathology.org, using the brain tumor classifier v12.5 and the meningioma classifier v2.4. The best match in the reports was subsequently used for further classification. CNV profiles were inferred from the EPIC methylation essay. Assessment of homozygous deletion of cyclin-dependent kinase inhibitors 2A/B (CDKN2A/B) was based on CNV profiles and additional visual judgement. Chromosomal arm deletions and gains were assessed using the CNV profile as previously reported.[16] The integrated molecular-morphological risk score was calculated as previously reported.[14]

MRI Processing and Feature Extraction

All patients underwent a cranial MRI prior to surgery. MR images were acquired on different MR machines, and image acquisitions ranged from 2D to 3D acquisitions.

We extracted the preoperative baseline MRI, including T2-weighted images (T2w), fluid attenuated inversion recovery (FLAIR), T1-weighted images without (T1w) as well as with contrast enhancement (T1w-ce) for all patients. In some cases, sequences were missing (either T2w or T1w). In these cases, we used a pretrained Deep Learning-based Generative Adversarial Network to synthesize these missing sequences to allow for automatic segmentation as described earlier.[17] Diffusion-weighted imaging was also missing in a relevant subset of patients. T1w-ce images were available for all cases and were never synthesized, thus feature extraction was focused on T1w-ce to minimize possible interfering factors.

Automated meningioma segmentation was performed by co-registering the respective MRI scans into SRI24 atlas space using NiftyReg.[18,19] After brain extraction with HD-BET, automated tumor segmentation was performed using the open-source BraTS Toolkit developed by our group.[20,21] The BraTS Toolkit segments each tumor into necrotic areas, contrast-enhancing tumor, and edema. These automated segmentations were checked (and corrected where necessary) by a board-certified neuroradiologist (O.K.) with over 10 years of brain tumor imaging experience using ITK-SNAP (version 3.8).[22]

To quantify image features, the T1w-ce images were *Z*-score normalized according to recommendation, discretized to a bin width of 0.1 and radiomics feature extraction was performed using the open-source package *PyRadiomics* (version 3.1.0) in Python.[23,24] This way, 3 basic groups of radiomics features were extracted from T1w-ce images according to the image biomarker standardization biomarker definition, including 16 shape, 19 first order, and 24 texture features from a gray level co-occurrence matrix (GLCM) from the "tumor core" mask, that is, necrotic/cystic or contrast-enhancing tumors.[25]

Machine Learning Classifier

To predict the IRS class (low-risk, medium-risk, high-risk), or a simplified version, where medium- and high-risk classes were combined as high-risk (binary classification) by the aforementioned selected radiomics features, we employed the random forest classifier implemented in the *pycaret* package (version 3.0.4).[26] Random forest is an ensemble classifier that aggregates voting from a large number of (ideally uncorrelated) decision trees through repeatedly training single weak classifiers from the original data through resampling with replacement. To avoid overfitting the machine learning (ML) model to the available data, default settings were used for the random forest parameters. The entire data set was split (stratified by IRS class) into a training set ($n = 120$ patients) and a hold-out test set ($n = 40$ patients) only used for the final evaluation. Besides the classification result, random forest also estimated feature importance, that is, the individual contribution of each feature to the final classification. This allows to investigate classifier decisions and understand the most meaningful features.

Statistical Analysis

Descriptive statistics for patient characteristics were reported as mean ± standard deviation (SD), median, and range. Mann–Whitney *U* test (for 2 groups) and Kruskal–Wallis *H* test (for 3 groups) or Chi-square test (categorical data) were used to compare parameters, respectively. All statistical tests were performed 2-sided and a p value < .05 was considered statistically significant.

Results

Patients' Characteristics

Our study comprised a total of 160 preoperative meningioma patients from 2 university centers, further referred to as cohort 1 ($n = 67$ patients) and cohort 2 ($n = 93$ patients). Table 1 lists important patient characteristics. Regarding age and sex, both cohorts were equally distributed. Cohort 1 included several WHO grade 3 meningioma patients ($n = 6$). Since WHO grade is one of 3 attributes relevant for the integrated risk score (IRS) (see Methods for details), cohort 1 tended to have higher IRSs, although this difference was not statistically significant. Note, however, that for separating patients into train or test cohorts, we stratified sampling explicitly for the IRS category.

IRS Classification

Multiclass IRS classification based on preoperative T1w-ce features reached a test set accuracy of 65% (26/40 patients correctly classified) at an area under the curve (AUC) of 0.7. As evident from the confusion matrix shown in Table 2a, this is mostly driven by the inability to learn reliable decision boundaries around medium-risk patients, particularly between medium-risk and high-risk, suggesting a rather continuous (but directed) change of imaging phenotype with increasing IRS. In line with this observation, there were only few misclassifications between low- and high-risk. One of the strengths of random forests is use of sample and feature bagging. However, this inherent randomness can lead to variations in the classifier results. To better understand the stability of our model, we reran the random forest classifier 1000 times (using the same train/test split). Across these 10 runs, the median AUC was 0.73 (interquartile range: 0.7–0.74), indicating good model stability.

Table 1. Patient Characteristics

Attribute	Cohort 1 (*n* = 67 patients)	Cohort 2 (*n* = 93 patients)
Age (median ± IQR)	66 years (51–76)	61 years (48–72)
Sex (*n*)	33 male/34 female	38 male/55 female
WHO grade (*n*)	61 grade 2/6 grade 3	93 grade 2
Integrated risk score (median ± IQR)	5 (3–6)	5 (1–5)
Integrated risk score category (*n*)	14 low-risk/34 medium-risk/19 high-risk	28 low-risk/51 medium-risk/14 high-risk

IQR = interquartile range.

Table 2. Results of the Different Machine Learning Classifiers

True class	Predicted class		
(a)	Low-risk	Medium-risk	High-risk
Low-risk	8	3	0
Medium-risk	2	18	1
High-risk	1	7	0
(b)	Not high-risk	High-risk	
Not high-risk	31	1	
High-risk	7	1	
(c)	Not low-risk	Low-risk	
Not low-risk	28	1	
Low-risk	3	8	

Results of the different machine learning classifiers developed by a random forest classifier tested in 40 patients. Multiclass classifier for IRS (a) and binary classifiers for low-risk (b), and high-risk prediction (c).

We therefore explored 2 further classification tasks to circumvent this: For the first task, we grouped low-risk and medium-risk patients as "not-high-risk" and trained a classifier to differentiate these from high-risk patients. This classifier had a test set accuracy of 80% (32/40 patients correctly classified; Table 2b), but a low AUC of 0.6. The low classification performance here was mostly driven by the inability to correctly identify a predictive imaging signature for high-risk patients.

We then grouped medium-risk and high-risk patients as "non-low-risk" and contrasted them with low-risk patients. This classifier had a high test set accuracy of 90% (36/40 patients correctly classified; Table 2c) with 0.88 AUC. Importantly, only one case was wrongly classified as "low-risk" (in fact medium-risk), resulting in a positive predictive vale (PPV, Precision) of 88.8% and a negative predictive value (NPV) of 90%.

Imaging Features Differentiating IRS Groups

To better characterize the morphologic differences underlying the classification results, we investigated the feature importances for all 3 models (Figure 1). Of particular relevance, shape features describing the roundness of tumors (most prominently, sphericity) were strongly influential for the IRS prediction and low-risk classification. To further investigate this, we compared sphericity between tumors of different IRS grades. Sphericity directly measures the roundness of the shape of the tumor relative to a sphere. It ranges between 0 and 1, where higher values indicate higher roundness (1 would mean a perfect sphere). Strikingly, we found a clear decrease in sphericity with increasing IRS grade, and this finding was concordantly seen in both data sets (Figure 2; p value < .001, Kruskal–Wallis H test). In more detail, the sphericity of low-risk tumors was significantly larger than both medium-risk ($p < .001$, Mann–Whitney U test) and high-risk tumors ($p < .001$, Mann–Whitney U test). In line with our observation that medium- and high-risk are not easily separable, the difference between them; however, did not formerly met statistical significance ($p = .052$, Mann–Whitney U test). This difference in shape can also be identified visually (Figure 3).

Discussion

A molecularly integrated grading scheme for meningiomas demonstrated an improved prediction accuracy of progression-free survival when compared to the current WHO grading system (c-index, $p = .004$; prediction error at 5 and 10 years, $p = .0021$ and $p = .0001$, respectively).[5,14] IRS has been demonstrated to enhance diagnostic accuracy, which is especially of interest to WHO grade 2 and 3 meningiomas with a benign follow-up.

Despite its clear clinical superiority, widespread implementation of this classifier requires routine epigenetic profiling, which is associated with costs and required infrastructure as well as expertise. Alternatively, the imaging-based classification of meningiomas, as described here, offers a compelling option, especially for retrospectively analyzing data sets. We found that, in particular, molecularly low-risk WHO grade 2 and 3 meningiomas can be classified with a very high accuracy in a heterogeneous, multicentric cohort. This is of clinical relevance, as a recent analysis of the clinical course of WHO grade 2 meningioma suggested that these low-risk groups indeed have an excellent clinical outcome (as opposed to high-risk, and to a lesser extent also medium-risk).[27] This makes the reliable distinction between these molecular risk profiles very important for a personalized clinical decision-making. However, further studies, including clinical follow-up are needed to investigate clinical significance.

A recent systematic review on meningioma radiomics found a robust correlation with meningioma grading according to WHO grading criteria and biological features, yielding a mean AUC of 0.851 ± 0.078 and 0.89 ± 0.07, respectively.[28] In this study, the majority of models also sorted meningiomas into low (WHO grade 1) versus high (WHO grade 2–3) grade. However, biological features only focused on meningioma firmness, fibrous quality, and Ki-67.[28] Our data further support these findings, as we could in particular predict patients with a low-risk profile with very high test set accuracy of >90%. Interestingly, we observed that when performing a multiclass classification, the resulting model mostly struggled with clearly separating medium-risk from high-risk tumors (Table 2a). On the other hand, there were only comparatively few cases of misclassifications between high- and low-risk patients. Combined with our observation of reduced sphericity correlating with increasing IRS grade, seen consistently in both cohorts, this indicates the presence of a discernible imaging phenotype continuum across IRS grades. A classifier can learn this continuum, particularly for identifying low-risk tumors. Our results align well with the clinical observations from Deng et al., who noted a significantly better outcome for low-risk WHO grade 2 meningiomas, while medium- and high-risk tumors shared a similar clinical course.[27]

For the extraction of radiomic features, reliable and reproducible segmentation of tumors is of paramount importance.

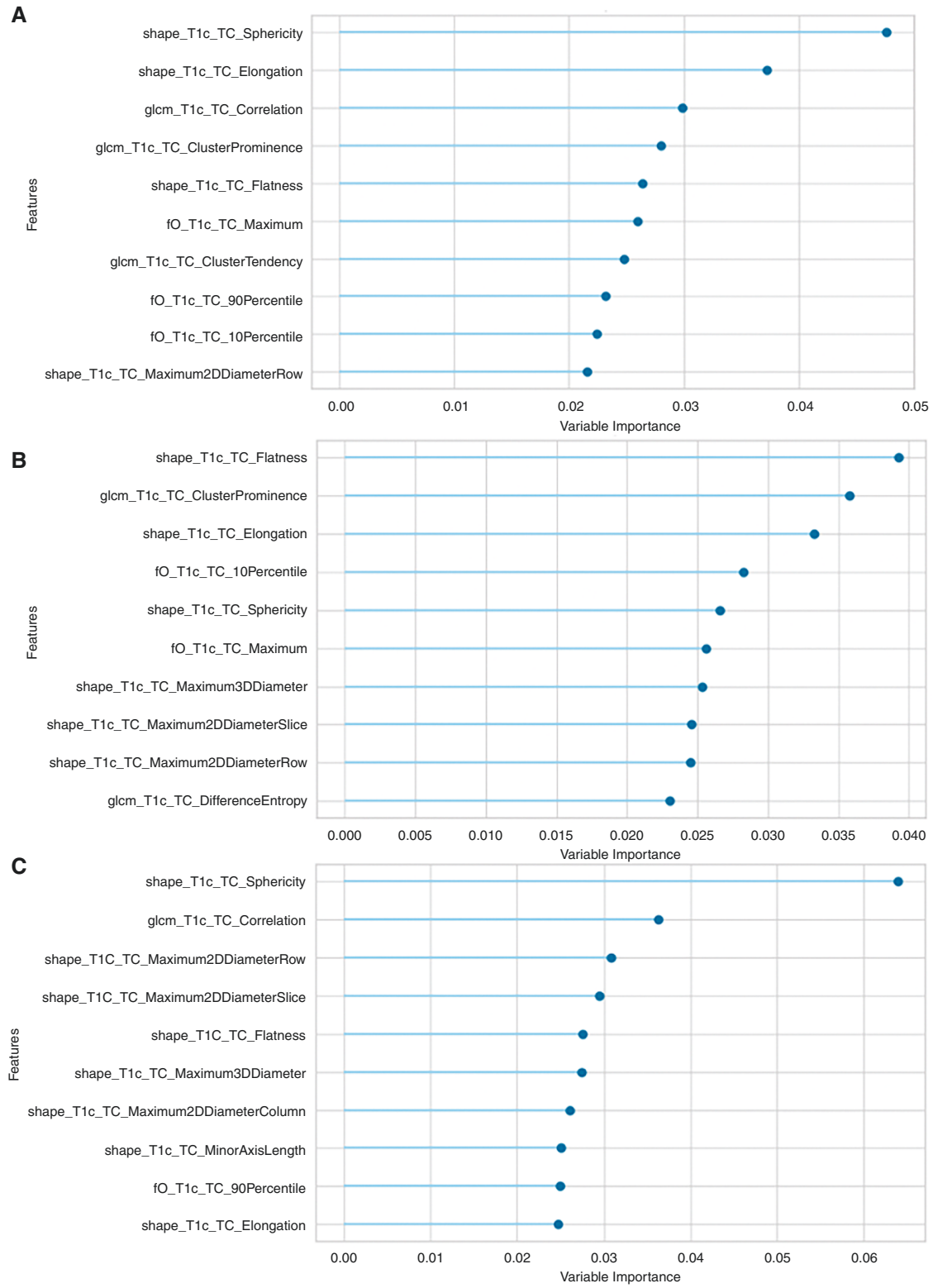

Figure 1. Importances of the top ten different radiomic features in the different models. Importances of different radiomic features in the different models. Shape features were strongly influential for the IRS prediction (a) and low-risk classification (c) compared to high-risk prediction (b).

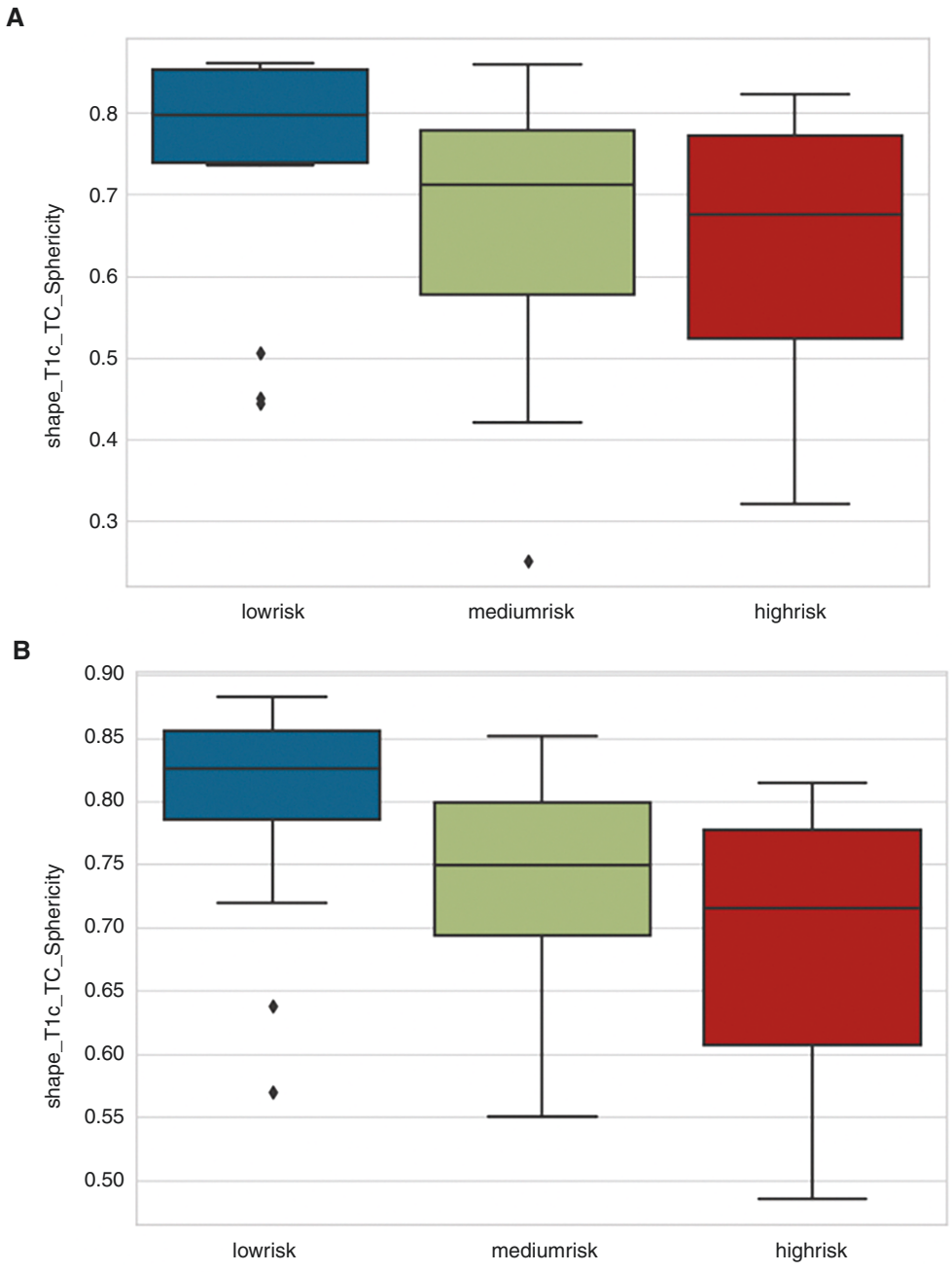

Figure 2. Box plots of shape features for IRS prediction in both university centers cohorts. Decrease in sphericity with increasing IRS grade was found in both data sets of the university center cohorts (a and b, respectively; *p* value < .001, Kruskal–Wallis *H* test).

In recent years, advances in deep learning-based automated tumor segmentation algorithms have led to the development of models, which now segment complex tumors (like gliomas) at the level of expert human raters.[29,30] To avoid manual segmentation, we employed an ensemble model of glioma segmentation algorithms using our self-developed BraTS (BrainTumor Segmentation)Toolkit, which is also freely available.[21]Though developed for gliomas, this ensemble segmentation model worked very well in our experience also for meningiomas, with only very little manual correction necessary. In this year's version of the BraTS challenge, there is a dedicated subchallenge for meningioma segmentation. We anticipate that this will lead to the availability of segmentation algorithms specifically targeted at meningiomas, which will prospectively further improve the fully automated segmentation (and subsequently, feature extraction and classification) and might thus further advance the applicability of imaging-based IRS prediction in clinical routine.[31]

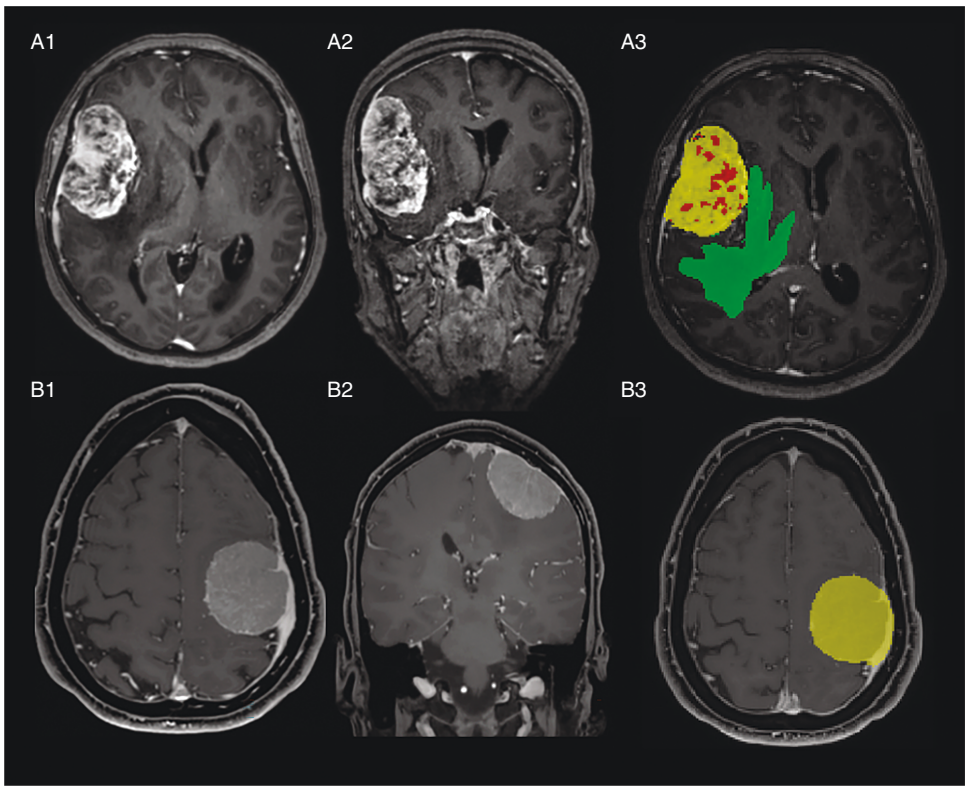

Figure 3. (A) Example of a patient with a meningioma WHO grade 2 and high-risk IRS profile. Axial and coronal T1WI + CE show low sphericity of the contrast-enhancing tumor. Segmentation shows contrast-enhancing tumor (yellow), necrotic area (red), and peritumoral edema (green). (B) Example of a patient with a meningioma WHO grade 2 and low-risk IRS profile. Axial and coronal T1WI + CE show high sphericity of the contrast-enhancing tumor. Segmentation shows contrast-enhancing tumor (yellow).

In addition to basic MRI sequences, advanced MRI techniques, such as diffusion imaging and MR-perfusion, may provide additional information and should be evaluated in the future. In higher-graded meningiomas, ADC may be relatively low and high relative cerebral blood flow (rCBF) in arterial spin labeling (ASL) perfusion can be found in certain meningioma subtypes.[32] Another study by Zhang et al. suggests that relative cerebral blood volume (rCBV) values in peritumoral edemas are significant enough to differentiate benign from malignant meningioma.[33,34]

One distinct advantage of machine learning classifiers, like the random forest we used, over deep learning classifiers is their enhanced explainability. This is due to the manual crafting of features and the ability to evaluate feature importances, allowing for the identification of which aspects of the imaging phenotype contribute most to the classification. Our finding of decreasing sphericity with higher IRS grades has immediate clinical applicability (Figure 3). In particular, for cases with an "en plaque" or irregular growth pattern, a high-risk (or medium-risk) molecular profile is very likely.

Our retrospective study has several limitations. Despite being carried out across 2 centers with imaging data from different scanners (often times, external MR images were used preoperatively), a validation in larger, heterogeneous data sets is missing. The role of sphericity in more benign cases could have been further supported by including WHO grade 1 meningiomas. However, we excluded them in advance, in order to focus our results on higher-grade meningiomas, as further treatment decisions are more likely to be considered in this subgroup. Along this line, only 6 WHO grade 3 meningiomas were included. Further, in order to perform automatic segmentation, skullstripping needed to be performed (this will also be the case for the BraTS meningioma challenge). While this approach may result in missing intraosseous parts of meningiomas for analysis, we believe the benefits of reliable automated tumor segmentation outweigh this limitation. Besides, our data lacks clinical follow-up information including progression-free surivival and overall survival as these would be of interest to be compared with radiomic features directly. Furthermore, as discussed above, advanced imaging sequences might further improve classification. In particular, diffusion and perfusion imaging hold promise, but also somatostatin-receptor PET. These sequences could be particularly useful in distinguishing between medium- and high-risk tumors. While for this study, we focused on using a random forest classifier to avoid potential issues of "over-optimization" that may arise from testing multiple classifier methods, another potential line of research is the in-depth comparison of different ML classifiers (regression, support vector machine, etc.) and compare their

effectiveness in capturing the underlying meningioma biology from imaging data.

Conclusion

Our study provides first evidence for a machine learning classifier to noninvasively predict the molecular risk profile of WHO grade 2 and 3 meningiomas. Validation in larger data sets as well as future studies are warranted to gain further insights into its possible role in the interplay of molecular grading, therapy decisions, and clinical course.

Keywords

Integrated risk score | Meningioma | Neuro-oncology | Radiomics

Lay Summary

Meningiomas are common tumors that grow from the brain's protective covering. Most are slow-growing, but some can be more aggressive. At present, the only method to reliably tell if a meningioma is aggressive is through pathology and genetic testing of the tumor removed with surgery. The authors in this study aimed to determine whether aggressiveness in meningioma could be predicted without surgery. To do this, they analyzed the MRI scans of 160 patients with higher-grade aggressive meningiomas before surgery. They developed computer models to predict meningioma aggressiveness using MRI data alone. Their results show that computer models that used MRI data alone could distinguish between low and high aggressive meningiomas with about 90% accuracy. It was more difficult for these models to distinguish between medium and highly aggressive meningiomas.

Funding

None declared.

Conflict of interest statement

None declared.

Authorship statement

Data collection and analysis: O.K., C.D., F.S., F.E., D.C., D.K., D.B., and B.W. Interpretation of analysis: all authors. Drafting of the initial manuscript: O.K., C.D., D.K., D.B., and B.W. Reviewing, editing, and approval of final manuscript: all authors.

Affiliations

Department of Diagnostic and Interventional Neuroradiology, School of Medicine, Klinikum rechts der Isar, Technical University of Munich, Munich, Germany (O.K., M.G., M.-C.M., C.Z., B.W.); Department of Neuropathology, School of Medicine, Institute of Pathology, Technical University of Munich, Munich, Germany (C.De); Department of Neuropathology, Institute of Pathology, University Hospital Heidelberg, Heidelberg, Germany (F.S.); Clinical Cooperation Unit Neuropathology, German Cancer Consortium (DKTK), German Cancer Research Center (DKFZ), Heidelberg, Germany (F.S.); Department of Radiation Oncology, Charité – Universitätsmedizin Berlin, Corporate Member of Freie Universität Berlin and Humboldt-Universität zu Berlin, Berlin, Germany (F.E., G.A., D.Z., D.K.); German Cancer Consortium (DKTK), Partner Site Berlin, German Cancer Research Center (DKFZ), Heidelberg, Germany (F.E., D.C.); Department of Neuropathology, Charité – Universitätsmedizin Berlin, Corporate Member of Freie Universität Berlin and Humboldt-Universität zu Berlin, Berlin, Germany (D.C.); Department of Radiation Oncology, Klinikum rechts der Isar, Technische Universität München, Institut für Innovative Radiotherapy (iRT), Munich, Germany (J.C.P., C.Di, S.E.C., D.B.); Department of Neurosurgery, Technical University of Munich, School of Medicine, Klinikum rechts der Isar, Munich, Germany (C.N., B.M.); Department of Neurosurgery, University Hospital Heidelberg, Heidelberg, Germany (S.M.K.); Department of Neurosurgery, Charité – Universitätsmedizin Berlin, Corporate Member of Freie Universität Berlin and Humboldt-Universität zu Berlin, Berlin, Germany (G.A., J.O., P.V.); Department of Nuclear Medicine, Klinikum Rechts der Isar, Technical University of Munich, München, Germany (I.Y.); Faculty of Medicine, HMU Health and Medical University, Potsdam, Germany (D.K.); TranslaTUM, Center for Translational Cancer Research, Technical University of Munich, Munich, Germany (B.W.)

References

1. Wiemels J, Wrensch M, Claus EB. Epidemiology and etiology of meningioma. *J Neurooncol*. 2010;99(3):307–314.
2. Yang SY, Park CK, Park SH, et al. Atypical and anaplastic meningiomas: prognostic implications of clinicopathological features. *J Neurol Neurosurg Psychiatry*. 2008;79(5):574–580.
3. Pasquier D, Bijmolt S, Veninga T, et al.; Rare Cancer Network. Atypical and malignant meningioma: outcome and prognostic factors in 119 irradiated patients. A multicenter, retrospective study of the Rare Cancer Network. *Int J Radiat Oncol Biol Phys*. 2008;71(5):1388–1393.
4. Stessin AM, Schwartz A, Judanin G, et al. Does adjuvant external-beam radiotherapy improve outcomes for nonbenign meningiomas? A surveillance, epidemiology, and end results (SEER)-based analysis. *J Neurosurg*. 2012;117(4):669–675.
5. Driver J, Hoffman SE, Tavakol S, et al. A molecularly integrated grade for meningioma. *Neuro Oncol*. 2022;24(5):796–808.
6. Pettersson-Segerlind J, Fletcher-Sandersjöö A, von Vogelsang AC, et al. Long-term follow-up, treatment strategies, functional outcome, and health-related quality of life after surgery for WHO grade 2 and 3 intracranial meningiomas. *Cancers (Basel)*. 2022;14(20):5038.

7. Yao Y, Xu Y, Liu S, et al. Predicting the grade of meningiomas by clinical-radiological features: a comparison of precontrast and postcontrast MRI. *Front Oncol*. 2022;12:1053089.
8. Yi Z, Long L, Zeng Y, Liu Z. Current advances and challenges in radiomics of brain tumors. *Front Oncol*. 2021;11:732196.
9. Zhou H, Chang K, Bai HX, et al. Machine learning reveals multimodal MRI patterns predictive of isocitrate dehydrogenase and 1p/19q status in diffuse low- and high-grade gliomas. *J Neurooncol*. 2019;142(2):299–307.
10. Kickingereder P, Bonekamp D, Nowosielski M, et al. Radiogenomics of glioblastoma: machine learning-based classification of molecular characteristics by using multiparametric and multiregional MR imaging features. *Radiology*. 2016;281(3):907–918.
11. Choi YS, Bae S, Chang JH, et al. Fully automated hybrid approach to predict the IDH mutation status of gliomas via deep learning and radiomics. *Neuro Oncol*. 2021;23(2):304–313.
12. Singh G, Manjila S, Sakla N, et al. Radiomics and radiogenomics in gliomas: a contemporary update. *Br J Cancer*. 2021;125(5):641–657.
13. Ehret F, Kaul D, Clusmann H, Delev D, Kernbach JM. Machine learning-based radiomics in neuro-oncology. *Acta Neurochir Suppl*. 2022;134:139–151.
14. Maas SLN, Stichel D, Hielscher T, et al.; German Consortium on Aggressive Meningiomas (KAM). Integrated molecular-morphologic meningioma classification: a multicenter retrospective analysis, retrospectively and prospectively validated. *J Clin Oncol*. 2021;39(34):3839–3852.
15. Sahm F, Schrimpf D, Stichel D, et al. DNA methylation-based classification and grading system for meningioma: a multicentre, retrospective analysis. *Lancet Oncol*. 2017;18(5):682–694.
16. Hielscher T, Sill M, Sievers P, et al. Clinical implementation of integrated molecular-morphologic risk prediction for meningioma. *Brain Pathol*. 2023;33(3):e13132.
17. Thomas MF, Kofler F, Grundl L, et al. Improving automated glioma segmentation in routine clinical use through artificial intelligence-based replacement of missing sequences with synthetic magnetic resonance imaging scans. *Invest Radiol*. 2022;57(3):187–193.
18. Rohlfing T, Zahr NM, Sullivan EV, Pfefferbaum A. The SRI24 multichannel atlas of normal adult human brain structure. *Hum Brain Mapp*. 2010;31(5):798–819.
19. Modat M, Cash DM, Daga P, et al. Global image registration using a symmetric block-matching approach. *J Med Imaging (Bellingham)*. 2014;1(2):024003.
20. Isensee F, Schell M, Pflueger I, et al. Automated brain extraction of multisequence MRI using artificial neural networks. *Hum Brain Mapp*. 2019;40(17):4952–4964.
21. Kofler F, Berger C, Waldmannstetter D, et al. BraTS toolkit: translating BraTS brain tumor segmentation algorithms into clinical and scientific practice. *Front Neurosci*. 2020;14:125.
22. Yushkevich PA, Piven J, Hazlett HC, et al. User-guided 3D active contour segmentation of anatomical structures: significantly improved efficiency and reliability. *Neuroimage*. 2006;31(3):1116–1128.
23. Carré A, Klausner G, Edjlali M, et al. Standardization of brain MR images across machines and protocols: bridging the gap for MRI-based radiomics. *Sci Rep*. 2020;10(1):12340.
24. van Griethuysen JJM, Fedorov A, Parmar C, et al. Computational radiomics system to decode the radiographic phenotype. *Cancer Res*. 2017;77(21):e104–e107.
25. Zwanenburg A, Vallières M, Abdalah MA, et al. The image biomarker standardization initiative: standardized quantitative radiomics for high-throughput image-based phenotyping. *Radiology*. 2020;295(2):328–338.
26. Breiman L. Random forests. *Mach Learn*. 2001;45(1):5–32.
27. Deng MY, Hinz F, Maas SLN, et al. Analysis of recurrence probability following radiotherapy in patients with CNS WHO grade 2 meningioma using integrated molecular-morphologic classification. *Neurooncol. Adv*. 2023;5(1):vdad059.
28. Patel RV, Yao S, Huang RY, Bi WL. Application of radiomics to meningiomas: a systematic review. *Neuro Oncol*. 2023;25(6):1166–1176.
29. Whybra P, Spezi E. Sensitivity of standardised radiomics algorithms to mask generation across different software platforms. *Sci Rep*. 2023;13(1):14419.
30. Spyridon Bakas MR, Andras J, Stefan B, et al. Identifying the best machine learning algorithms for brain tumor segmentation, progression assessment, and overall survival prediction in the BRATS challenge. *ArXiv*. 2018 Nov 5. doi: 10.48550/arXiv.1811.02629.
31. LaBella D, Adewole M, Alonso-Basanta M, et al. The ASNR-MICCAI brain tumor segmentation (BraTS) challenge 2023: intracranial meningioma. *ArXiv [Preprint]*. 2023 May 12:arXiv:2305.07642v1.
32. Huang RY, Bi WL, Griffith B, et al. Imaging and diagnostic advances for intracranial meningiomas. *Neuro Oncol*. 2019;21(Suppl 1):i44–i61.
33. Zhang H, Rödiger LA, Shen T, Miao J, Oudkerk M. Perfusion MR imaging for differentiation of benign and malignant meningiomas. *Neuroradiology*. 2008;50(6):525–530.
34. Rohilla S, Garg HK, Singh I, Yadav RK, Dhaulakhandi DB. rCBV- and ADC-based grading of meningiomas with glimpse into emerging molecular diagnostics. *Basic Clin Neurosci*. 2018;9(6):417–428.